INFLUENCE OF DOPANT SPECIES ON ELECTRON MOBILITY IN InP

Ch. Köpf, G. Kaiblinger-Grujin, H. Kosina, and S. Selberherr

Institute for Microelectronics, TU Vienna
Gusshausstrasse 27–29, A-1040 Vienna, Austria

Introduction

We present a theoretical reassessment of electron mobility in doped InP with respect to different doping species. Using Thomas-Fermi theory in the energy functional formulation we describe the charge density of the individual impurity ion. Analytical expressions for the scattering rate are calculated based on a variational expression of Schwinger. Employing these results in a Monte Carlo calculation we find no significant dependence of mobility on doping species up to 10^{18} cm^{-3}. For higher concentrations an increasing difference is observed which reaches 25% at 10^{19} cm^{-3} for Si and Te doping.

I. Background

The dependence of the electron mobility μ on impurity concentration has been investigated for a long time by many theoretical approaches and experimental work mostly in n-InP. Many corrections to the simple Brooks-Herring (BH) model have been introduced improving the overall agreement with experiments [8]. All attempts in the past failed to explain the influence of the different dopant species characterized by the atomic number Z and electron number N. One usually assumes a delta-like impurity charge concentrated in the origin of the dopant ion neglecting the spatial extension of the electron charge distribution of the dopant. This is equivalent to neglecting the dependence of the atomic form factor $F(q)$ on the momentum transfer $q = |\mathbf{k}' - \mathbf{k}|$. We show that consideration of a spherically symmetric charge density of the electrons explains the different mobilities for majority and minority electrons for various dopants at high concentration.

II. Thomas-Fermi atomic model

Assuming a hydrogen-like electron charge distribution consisting of N valence electrons

$$\rho_e(r) = \frac{N \alpha^3}{8 \pi} e^{-\alpha r} \qquad (1)$$

$$N = \int \rho_e(r)\, dV$$

and a point-like nucleus with charge Z, the total charge distribution of an impurity ion (in units of the elementary charge e_0) is

$$\rho_{ion}(r) = Z\,\delta(r) - \rho_e(r). \qquad (2)$$

The atomic form factor $F(q)$ which is the fourier transform of ρ_e [11],

$$F(q) = \int \rho_e(r)\, e^{-i\,\mathbf{q}\cdot\mathbf{r}}\, dV = \frac{N\,\alpha^4}{\left(q^2 + \alpha^2\right)^2}, \qquad (3)$$

directly enters the effective scattering potential in momentum space $U(q)$

$$U(q) = V_0\, \frac{Z - F(q)}{q^2 + \beta^2} \qquad (4)$$

$$V_0 = \frac{2\,e_0^2\,m^*}{\hbar^2\,\varepsilon}.$$

β is the inverse Thomas-Fermi screening length. The reason for different scattering rates for different dopants lies in the different radial extension of their charge density expressed by the variational parameter α. To obtain numerical values for α as function of the doping species determined by Z and N we minimize the semiclassical Thomas-Fermi energy functional [2, 4, 15]. It should be noted that the form factor can also explain the difference between majority and minority electron mobility since, besides the completely different functional form, $Z - F(q)$ is larger than unity in the first and smaller in the second case. Only in the limit of small-angle scattering ($q \to 0$) the form factor equals the number of electrons, $F(0) = N$, and the BH Model is retained.

III. Scattering rates

In addition to the first scattering amplitude of the Born approximation

$$f_1(q) = U(q), \qquad (5)$$

an analytical expression for the second scattering amplitude $f_2(q)$ of the Born series can be obtained if we use the approximation $F(q) \approx F(0) = N$,

$$
\begin{aligned}
f_2(q) &= \frac{U_0{}^2}{q\,A(q)}\left(\mathrm{atan}\left(\frac{\beta q}{2\,A(q)}\right) + \frac{i}{2}\log\frac{A(q)+k\,q}{A(q)-k\,q}\right)\\
A(q) &= \sqrt{\beta^4 + 4\,\beta^2\,k^2 + k^2\,q^2}\\
U_0 &= \frac{2\,e_0^2\,m^*\,(Z-N)}{\hbar^2\,\varepsilon}.
\end{aligned}
\qquad (6)
$$

The squared total scattering amplitude gives the differential scattering cross section

$$\frac{d\sigma}{d\Omega}(q) = |f(q)|^2, \qquad (7)$$

the total scattering cross section for electrons in state k is

$$\sigma(k) = \frac{2\pi}{k^2}\int_0^{2k} |f(q)|^2\, q\, dq. \qquad (8)$$

In the usual first Born approximation (B1), which is valid for low doping concentrations, the total amplitude simply is the first term $f_{B1}(q) = f_1(q)$. In the second Born approximation (B2) the series is truncated at the second term and $f_{B2}(q) = f_1(q) + f_2(q)$. However, the series does not converge for small energies. Therefore we calculate the total scattering amplitude by employing the variational method of Schwinger [6, 12]. The scattering amplitude denoted by $f_S(q)$ can be expressed as

$$f_S(q) = \frac{f_1(q)}{1 - \dfrac{f_2(q)}{f_1(q)}}. \qquad (9)$$

It can be shown that using (9) the divergence of the second Born approximation for the cross section σ_{B2} that occurs at small energies at low concentration is avoided while with increasing concentration σ_S exceeds σ_{B2}, which is in agreement with numerical phase-shift results [7].

As the Friedel sum rule [13] has to be obeyed by the effective scattering potential, a correction for the screening parameter β has to be introduced which now also depends on Z and N.

The behavior of the Schwinger formula is shown for example in the calculated momentum scattering rate for low (Fig. 1) and high doping concentrations (Fig. 2), respectively. While the scattering rate for weakly n-doped material using the Schwinger model is about three orders of magnitude below B2 and even smaller

than the BH value, it lies above BH for highly n-doped but below for heavily p-doped material. Throughout the figures "Schwinger" denotes the use of Schwinger formula with $F(q) = N$ while the chemical symbols for the dopant elements in Figs. 4-6 imply the usage of the Schwinger model including $F(q)$.
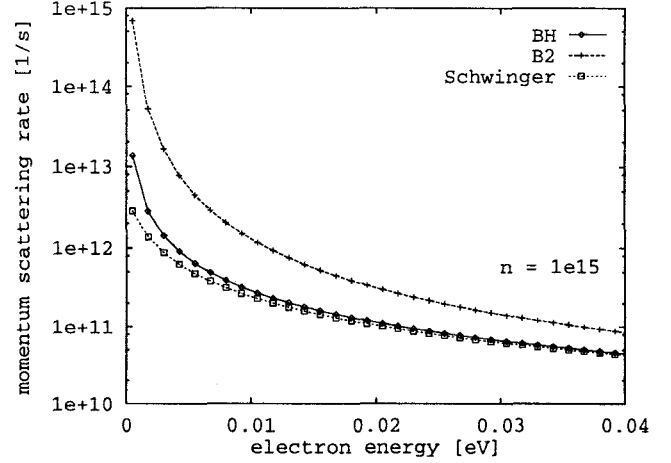

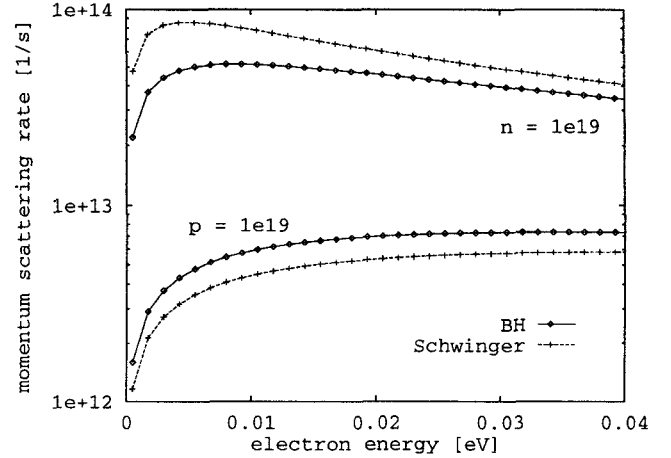Figure 1. Momentum scattering rate for a carrier concentration of 10^{15} cm^{-3} in InP with $F = F(0)$.

Figure 2. Momentum scattering rate for a carrier concentration of 10^{19} cm^{-3} in InP with $F = F(0)$.

IV. Monte Carlo Results

We employ the derived formulas in a single-particle Monte Carlo procedure to calculate the electron drift mobility at 300K using an analytic three-valley band dispersion and include phonon and plasmon scattering. At high concentrations many-body effects cause a distortion of the conduction band. The resulting concentration dependent change of the density of states

is incorporated via an increase of the effective electron mass. This mass enhancement is an increase of the band edge curvature mass and is not to be confused with the usual mass increase due to nonparabolicity. In analogy to [14] we model the effective mass by a polynomial in n,

$$\frac{m^*}{m_0}(n) = 0.075 + A\frac{n}{n_{ref}} + B\left(\frac{n}{n_{ref}}\right)^2 \quad (10)$$

$$A = 3.49 \times 10^{-3}$$
$$B = -2.37 \times 10^{-5}$$
$$n_{ref} = 10^{18}\,\mathrm{cm}^{-3}.$$

The coefficients have been obtained by a fit to experimental data summarized in [9]. Equation (10) is valid for $n < 3 \times 10^{19}$ cm^{-3}. The Pauli exclusion principle is accounted for by a rejection technique [3].

Fig. 3 compares the calculated majority mobility using the Brooks-Herring (BH) and "Schwinger" model with published experimental Hall data [1, 5, 9]. The Schwinger model reduces the overestimation of the mobility of BH at degenerate conditions significantly.
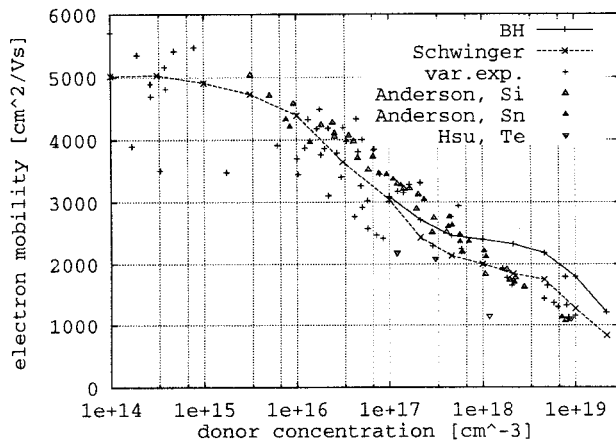

Figure 3. Majority electron mobility in InP with $F = F(0)$.

In Fig. 4 the mobility for different donors in InP is shown. We find no significant influence on Z up to $n \approx 10^{18}$ which is in agreement with experiments. With increasing concentration the different behavior becomes significant, heavier ions lead to lower values of μ. At 10^{19} cm^{-3} the mobility differs by 25% for [14]Si and [52]Te doping, which are the lightest respectively heaviest donors used. Unfortunately, the uncertainty and scattering of the available experimental data is of the same order of magnitude as the difference of the mobilities for various dopants. Hence, we are unable to assess the simulation results quantitatively at that time. In case of n-Si (Fig. 5), however, a systematic decrease of μ with increasing Z is observed experimentally, too [10].
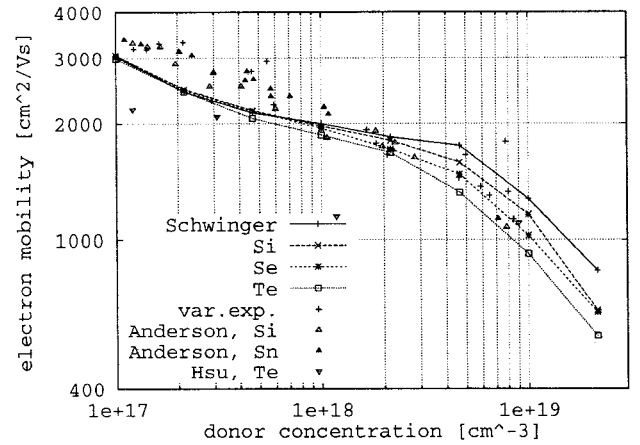

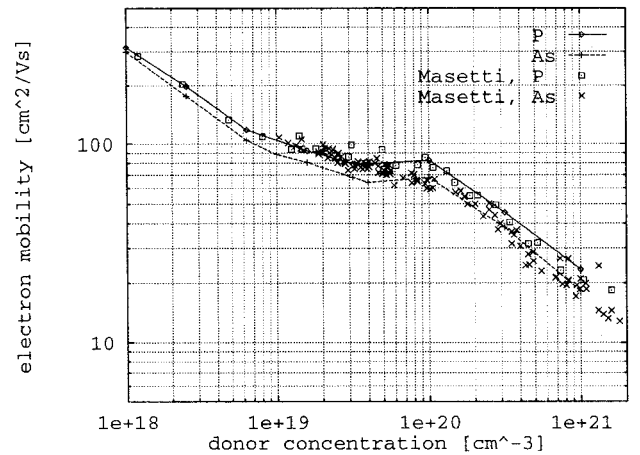Figure 4. Majority electron mobility in InP with $F = F(q)$.

Figure 5. Majority electron mobility in Si with $F = F(q)$.

Finally, Fig. 6 shows the well-known dip in μ in p-type material due to the plasmon interaction and a weaker dependence on Z compared to n-type material. Only for $p > 2 \times 10^{19}$ cm^{-3} a small difference is observed, μ again decreases with atomic number from [4]Be, [30]Zn to [48]Cd.

V. Conclusions

The proposed theoretical approach to our knowledge is the first physically based model to date which explains the dependence of the majority and minority electron mobility on various dopant species through the atomic number. Corrections to the first Born approximation are important for doping concentrations beyond 10^{17} cm^{-3}. The dependence on the donor species be-
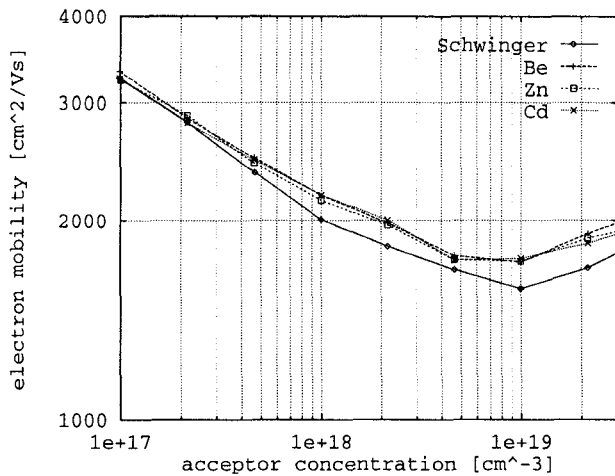
Figure 6. Minority electron mobility in InP with $F = F(q)$.

comes significant for concentrations beyond 10^{18} cm^{-3}. Neither compensation nor autocompensation is necessary to obtain a close agreement with experiment in highly n-degenerate material. In case of minority electron transport no species dependence is observed in the practical doping range.

References

[1] D.A. Anderson, N. Apsley, P. Davies, and P.L. Giles, "Compensation in Heavily Doped n-Type InP and GaAs", J. Appl. Phys., Vol. 58, No. 8, pp. 3059–3067, 1985.

[2] E. Fermi, "Un metodo statistico per la determinazione di alcune priorieta dell'atome", Rend. Accad. Naz. Lincei, Vol. 6, pp. 602–607, 1927.

[3] M.V. Fischetti and S.E. Laux, "Monte Carlo Analysis of Electron Transport in Small Semiconductor Devices Including Band-Structure and Space-Charge Effects", Phys. Rev. B, Vol. 38, No. 14, pp. 9721–9745, 1988.

[4] P. Gombas, Die statistische Theorie des Atomes und ihre Anwendungen. Springer, Wien, 1949.

[5] C.C. Hsu, J.S. Yuan, R.M. Cohen, and G.B. Stringfellow, "Doping Studies for InP Grown by Organometallic Vapor Phase Epitaxy", J. Cryst. Growth, Vol. 74, No. 3, pp. 535–542, 1986.

[6] Ch.J. Joachain, Quantum Collision Theory. North-Holland, Amsterdam, 1975.

[7] T. Kato, "Note on Schwinger's Variational Method", Prog. Theor. Phys., Vol. 6, No. 3, pp. 295–305, 1951.

[8] D. Lancefield, A.R. Adams, and M.A. Fisher, "Reassessment of Ionized Impurity Scattering and Compensation in GaAs and InP Including Correlation Scattering", J. Appl. Phys., Vol. 62, No. 6, pp. 2342–2359, 1987.

[9] M. Landolt and J. Börnstein, Numerical Data and Functional Relationships in Science and Techology. New Series, Group III, Vol. 22/A, Springer, Berlin, 1987.

[10] G. Masetti, M. Severi, and S. Solmi, "Modeling of Carrier Mobility Against Carrier Concentration in Arsenic-, Phosphorus- and Boron-Doped Silicon", IEEE Trans. Electron Devices, Vol. ED-30, No. 7, pp. 764–769, 1983.

[11] N.F. Mott and H.S.W. Massey, The Theory of Atomic Collisions. Clarendon Press, Oxford, 1949.

[12] J. Schwinger, "A Variational Principle for Scattering Problems", Phys. Rev., Vol. 72, No. 8, p. 742, 1947.

[13] F. Stern, "Friedel Phase-Shift Sum Rule for Semiconductors", Phys. Rev., Vol. 158, No. 3, pp. 697–698, 1967.

[14] D.M. Szmyd, P. Porro, A. Majerfeld, and S. Lagomarsino, "Heavily Doped GaAs:Se. I. Photoluminescence Determination of the Electron Effective Mass", J. Appl. Phys., Vol. 68, No. 5, pp. 2367–2375, 1990.

[15] L.H. Thomas, "The Calculation of Atomic Fields", Proc. Camb. Philos. Soc., Vol. 23, pp. 542–548, 1927.

Acknowledgments